Publications of The Korean Astronomical Society
26: 21 ∼ 33, 2007

MATRIX ELEMENTS AND CROSS SECTION OF RAMAN SCATTERING BY ATOMIC HYDROGEN[1]

Hee-Won Lee
Department of Astronomy and Space Science
Astrophysical Research Center for the Structure and Evolution of the Cosmos
Sejong University, Seoul, 143-747, Korea
E-mail: hwlee@sejong.ac.kr
(Received March 15, 2007; Accepted March 22, 2007)

ABSTRACT

Ever since the identification of 6830 and 7088 features as the Raman scattered O VI 1032, 1038 resonance doublets in symbiotic stars by Schmid (1989), Raman scattering by atomic hydrogen has been a very unique tool to investigate the mass transfer processes in symbiotic stars. Discovery of Raman scattered He II in young planetary nebulae (NGC 7027, NGC 6302, IC 5117) allow one to expect that Raman scattering can be an extremely useful tool to look into the mass loss processes in these objects. Because hydrogen is a single electron atom, their wavefunctions are known in closed form, so that exact calculations of cross sections are feasible. In this paper, I review some basic properties of Raman scattered features and present detailed and explicit matrix elements for computation of the scattering cross section of radiation with atomic hydrogen. Some astrophysical objects for which Raman scattering may be observationally pertinent are briefly mentioned.

Key Words: radiative transfer — scattering — binary:symbiotic — line:formation

I. INTRODUCTION

Raman scattering by atomic hydrogen was first proposed by Schmid (1989), who identified the mysterious emission features so-called "symbiotic bands" at 6830 Å and 7088 Å. Symbiotic stars are believed to be wide binary systems of a giant and a hot white dwarf, where the binary separation is too large for the cold component to fill the Roche lobe (e.g. Kenyon 1986). These broad emission features are observed only in symbiotic stars, where high excitatioin lines are also seen. Allen (1980) provided phenomenological properties of these unidentified lines that should be plausibly related with highly ionized species.

According to Schmid (1989), these optical emission features redward of Hα are originated from O VI 1032, 1038 resonance doublets that are incident from the hot component on to the thick H I region around the mass losing giant component. The hydrogen atom in the ground 1 state is excited into one of infinitely many p states including both bound and unbound state, subsequently de-excited into $2s$ state with the re-emission of an optical photon redward of Hα. The scattering process is schematically illustrated in Fig. 1.

Raman scattered O VI 6830 and 7088 are quite strong in symbiotic stars and exhibit rich structures in profiles and polarization (e.g. Harries & Howarth 1996, Schmid & Schild 1994). More specifically in a few D type symbiotics including RR Tel, V1016 Cyg and HM Sge the profiles are overall doubly peaked and the reddest part is linearly polarized in the direction perpendicular to that of the main part. The double-peak profile with polarization flip on the far red wing regions is consistent with the accretion disk emission model proposed by Lee & Park (1999).

The operation of Raman scattering of O VI 1032, 1038 doublets requires the existence of a thick H I region with H I column density $N_{HI} = 10^{23}$ cm^{-2}, which is quite a stringent condition. The co-existence of a thick neutral region and a strong UV emission region appears to be possible only in symbiotic stars, which explains the exclusive existence of 6830 and 7088 features in these objects.

[1]INVITED REVIEW

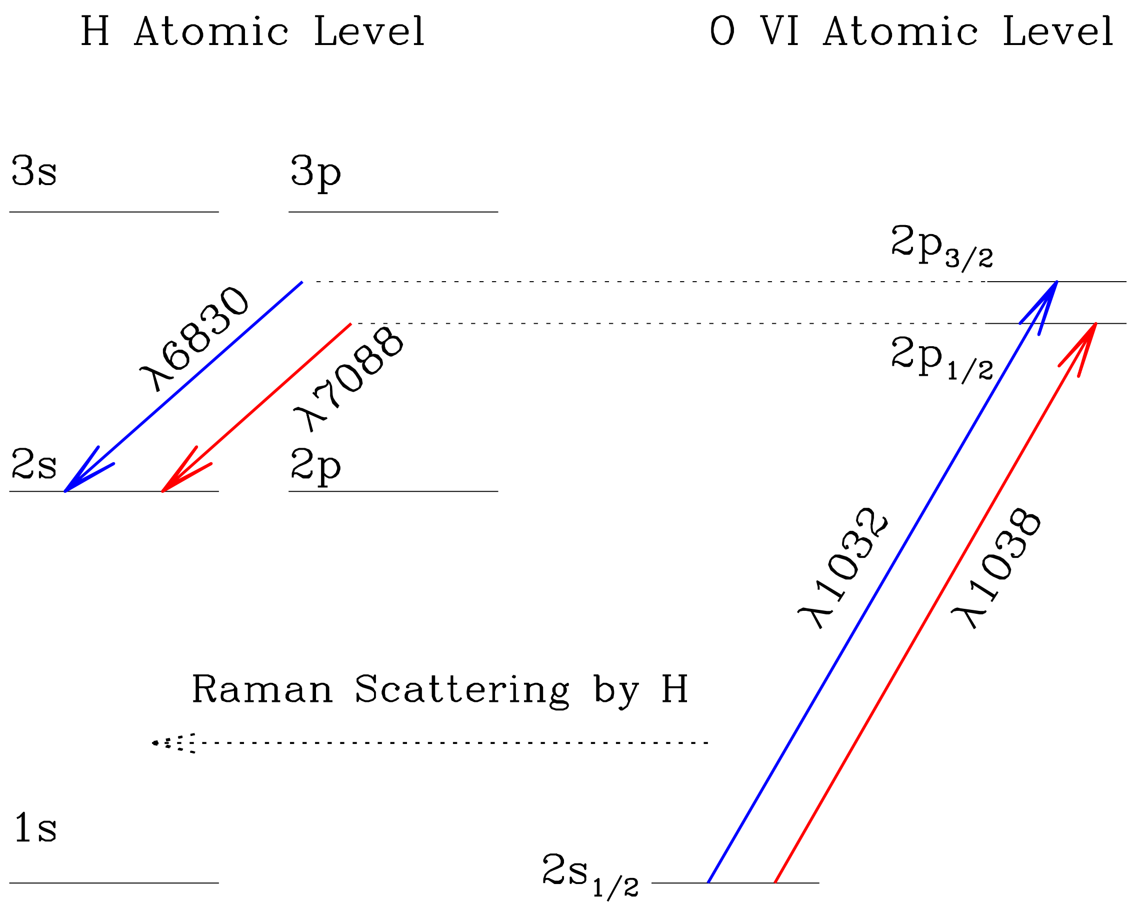

Fig. 1.— A schematic diagram to show the operation of Raman scattering for resonance doublet O VI 1032 and 1038 to form Raman scattered 6830 and 7088 features.

A much less severe condition is levied upon the presence of Raman scattered He II features blueward of hydrogen Balmer emission lines. The relevant scattering cross section is of order 10^{21} cm^2, two orders of magnitude smaller than O VI 1032, 1038 doublet. Raman scattered He II features are reported in the symbiotic stars RR Tel, V 1016 Cyg, HM Sge, where Raman scattered O VI 6830 and 7088 are also strong (e.g. van Groningen 1993, Birriel 2004).

The operation of Raman scattering by atomic hydrogen in objects other than symbiotic stars was first reported by Péquignot et al. (1997) who discovered Raman scattered He II 4850 blueward of Hβ in the young planetary nebula NGC 7027 (see also Zhang et al. 2005). Subsequently, the same feature was found in the butterfly planetary nebula NGC 6302 by Groves et al. (2002). Lee et al. (2006) used their spectroscopic data using CFHT to find the Raman scattered He II 4850 and 6545 in the young and compact planetary nebula IC 5117.

As has been pointed many researchers, the detailed profiles and polarization structures exhibited by Raman scattered features show enormous information regarding the mass transfer and mass loss processes (e.g. Nussbaumer, Schmid & Vogel 1989, Schild & Schmid 1996, Lee & Lee 1997, Schmid 2001, Jung & Lee 2004). In order to infer the exact amount and kinematic properties of neutral material in these objects, one needs to calculate exact scattering cross sections. In this paper, we briefly review the atomic physics related with Raman scattering involving atomic hydrogen and present detailed matrix elements.

II. ATOMIC PHYSICS OF RAMAN SCATTERING

The interaction of electromagnetic fields with atomic electrons is described by second order time dependent perturbation theory (e.g. Sakurai 1967). The interaction terms $\mathbf{p}\cdot\mathbf{A}$ and $\mathbf{A}\cdot\mathbf{p}$ in the Hamiltonian describe the processes of the annihilation of the incident photon and creation of an outgoing photon, while the atomic electron suffers transition from initial to final states.

In summary, the scattering cross section is given by

$$\frac{d\sigma}{d\Omega} = r_0^2\left(\frac{\omega'}{\omega}\right)\left|m_e\omega\omega'\sum_I\left(\frac{(\mathbf{x}\cdot\epsilon^{(\alpha')})_{BI}(\mathbf{x}\cdot\epsilon^{(\alpha)})_{IA}}{E_I-E_A-\hbar\omega}+\frac{(\mathbf{x}\cdot\epsilon^{(\alpha)})_{BI}(\mathbf{x}\cdot\epsilon^{(\alpha')})_{IA}}{E_I-E_A+\hbar\omega'}\right)\right|^2, \tag{1}$$

which is called the Kramers-Heisenberg formula. Here, ω and ω' are angular frequencies of incident and outgoing radiation. $\epsilon^{\alpha}, \epsilon^{\alpha'}$ are polarization vectors associated with incident and outgoing photons. $r_0 = e^2/(m_e c^2)$ is the classical electron radius with e and m_e being electron charge and mass, respectively. B, I and A stand for the final, intermediate and initial state of the atomic electron. We take $A = 1s$, the ground state. Considering the dipole nature of the radiative processes $I = np, n'p$, where a natural number $n \geq 2$ represents a bound state and positive real number n' represents a continuum eigenstate. We are particularly interested in the case $B = 2s$, in which case energy conservation requires

$$\hbar\omega' = \hbar\omega - \hbar\omega_{Ly\alpha}, \tag{2}$$

where $\omega_{Ly\alpha}$ is the angular frequency corresponding to Lyα radiation.

Noting that we have to consider all the contribution from bound np states and continuum $n'p$ states, the summation sign in Eq. (1) should be taken as the combination of an infinite sum over $n = 2, 3, 4, \ldots$ and an integral over n'.

Solely for hydrogen and hydrogen-like ions, the exact wavefunctions are known in closed form, so that in this paper, we review the matrix elements involved in Eq. (1) and present their explicit forms from which relevant cross sections can be easily computed. The Wigner-Eckart theorem tells us that the angular part can be separately computed, leaving the integration of the radial part. It can be shown that after averaging over polarization

$$\sigma = \frac{8\pi}{3}r_0^2\left(\frac{\omega'}{\omega}\right)\left|m_e\omega\omega'\sum_I\left(\frac{< B \parallel r \parallel I >< I \parallel r \parallel A >}{E_I-E_A-\hbar\omega}+\frac{< B \parallel r \parallel I >< I \parallel r \parallel A >}{E_I-E_A+\hbar\omega'}\right)\right|^2. \tag{3}$$

In the following subsections we describe the matrix elements in the summation. We will consider the matrix elements involving bound np states and then those involving free $n'p$ states.

(a) Bound-Bound Transitions

It is a very well know in a typical quantum mechanics text that the radial wavefunction R_{nl} of a hydrogen atom is represented by associate Laguerre function. However, it is more useful to regard R_{nl} as a special form of a hypergeometric confluent function, in which case

$$R_{nl}(r) = \frac{1}{(2l+1)!}\sqrt{\frac{(n+l)!}{(n-l-1)!2n}}\left(\frac{2Z}{n}\right)^{3/2}e^{-\frac{Zr}{n}}\left(\frac{2Zr}{n}\right)F(-(n-l-1), 2l+2, \frac{2Zr}{n}). \tag{4}$$

Here, the hypergeometric function $F(\alpha, \beta, \gamma; z)$ is defined as

$$F(\alpha,\beta,\gamma;z) = 1 + \frac{\alpha\beta}{\gamma}z + \frac{\alpha(\alpha+1)\beta(\beta+1)}{\gamma(\gamma+1)}\frac{z^2}{2!} + \cdots. \tag{5}$$

Nice recursion formulas involving hypergeometric functions let us write the radial matrix elements in a very general form, which is described in detail by Bethe & Salpeter (1957).

Many researchers carried out the detailed calculations of matrix elements related with Raman scattering (e.g. Saslow & Mills 1969). In this paper, we start with the matrix elements for bound-bound state transition, introduced by Karzas & Latter (1961), which is written as

$$\begin{aligned}\tau_{nl}^{n'l-1} &= \;< nl \parallel r \parallel n'l-1 > \int_0^\infty R_{n'l-1}(r) R_{nl} r r^2 dr \\ &= \frac{2^{2l}}{(2l-1)!}\left[\frac{(n+l)!(n'+l-1)!}{(n-l-1)!(n'-l)!}\right]^{1/2}(nn')^{l+1}(n+n')^{-n-n'}(n-n')^{n-2-l}(n'-n)^{n'-l} \\ &\times \left\{F(-n+l+1, l-n', 2l, \frac{-4nn'}{(n-n')^2}) - \left(\frac{n-n'}{n+n'}\right)^2 F(-n+l-1, l-n', 2l, \frac{-4nn'}{(n-n')^2})\right\}. \qquad (6)\end{aligned}$$

In this subsection only n' is a natural number greater than 1.

From a direct substitution for $n' = 1, l = 1$, we obtain

$$\begin{aligned}< 1s \parallel r \parallel np > &= 4\left[\frac{(n+1)!1!}{(n-2)!0!}\right]^{1/2} n^2 (n+1)^{-n-1}(n-1)^{n-3} \\ &\times \left\{F(-n+2, 0, 2, -\frac{4n}{(n-1)^2}) - \left(\frac{n-1}{n+1}\right)^2 F(-n, 0, 2, -\frac{4n}{(n-1)^2})\right\} \\ &= 2^4 n^{7/2}\frac{(n-1)^{n-5/2}}{(n+1)^{n+5/2}}. \qquad (7)\end{aligned}$$

Likewise, if we set $n' = 2, l = 1$, we have

$$\begin{aligned}< 2s \parallel r \parallel np > &= 4\left[\frac{(n+1)!2!}{(n-2)!(2-1)!}\right]^{1/2} \frac{(2n)^2(n-2)^{n+2-4}}{(n+2)^{n+2}} \\ &\times \left\{F(-n+2, -1, 2, \frac{-8n}{(n-2)^2}) - \left(\frac{n-2}{n+2}\right)^2 F(-n, -1, 2, \frac{-8n}{(n-2)^2})\right\} \\ &= 2^{17/2} n^{7/2}\sqrt{n^2-1}\frac{(n-2)^{n-3}}{(n+2)^{n+3}} \qquad (8)\end{aligned}$$

For $n' = 3, l = 1$ we have

$$\begin{aligned}\tau_{3s}^{np} &= 4\left[\frac{(n+1)!3!}{(n-2)!(3-1)!}\right]^{1/2} \frac{(3\;n)^2(n-3)^{n+3-4}}{(n+3)^{n+3}} \\ &\times \left\{F(-n+2, -2, 2, \frac{-12n}{(n-3)^2}) - \left(\frac{n-3}{n+3}\right)^2 F(-n, -2, 2, \frac{-12n}{(n-3)^2})\right\}. \qquad (9)\end{aligned}$$

After some algebraic manipulation (or using a symbolic computing software) one can show that the confluent hypergeometric function part can be simplified into

$$F(-n+2, -2, 2, \frac{-12n}{(n-3)^2}) - \left(\frac{n-3}{n+3}\right)^2 F(-n, -2, 2, \frac{-12n}{(n-3)^2}) = \frac{12n}{(n+3)^2(n-3)^3}\left[(7n^2-27)(n+3)\right]. \qquad (10)$$

This result is substituted into Eq. (9) to yield

$$\tau_{3s}^{np} = 3\sqrt{3}12^2 n^{7/2}\sqrt{n^2-1}(7n^2-27)\frac{(n-3)^{n-4}}{(n+3)^{n+4}}. \qquad (11)$$

Now in order to obtain the matrix elements between $3d$ and np states, we set $n \rightarrow n'$ and $l = 2, n = 3$ to obtain

$$\begin{aligned}
\tau_{3d}^{np} &= < 3d \parallel r \parallel np >= \frac{1}{4 \cdot 3!}\sqrt{\frac{5!(n+2-1)!}{0!(n-2)!}}\frac{(12n)^3(n-3)^{n+3-6}}{(n+3)^{n+3}} \\
&\times \left\{ F(0, -n+2, 4, \frac{-12n}{(3-n)^2}) - \left(\frac{n-3}{n+3}\right)^2 F(-2, -n+2, 4, \frac{-12n}{(3-n)^2}). \right\}
\end{aligned} \quad (12)$$

The confluent hypergeometric function part can be simplified by

$$\{\} = -\frac{6n^2}{5(n+3)^2(n-3)}. \quad (13)$$

With this simplification we finally obtain

$$< 3d \parallel r \parallel np >= -\frac{12^3\sqrt{3}}{\sqrt{10}} n^{11/2}\sqrt{n^2-1}\frac{(n-3)^{n-4}}{(n+3)^{n+4}}. \quad (14)$$

(b) Bound-Free Transitions

Analytic continuation can be done for R_{nl} to extend its domain into the complex plane, from which we obtain free state eigenfunctions. According to Bethe & Salpeter (1957) the wavefunction for the continuum states $n'p$ is given by

$$R_{n'l=1} = \frac{2[1+n'^2]^{1/2}}{[1-e^{-2\pi n'}]^{1/2}}\frac{n'^2}{4r^2}\frac{1}{2\pi}\int e^{-2ir\xi/n'}(\xi+\frac{1}{2})^{-in'-2}(\xi-\frac{1}{2})^{in'-2}d\xi. \quad (15)$$

The matrix element for a dipole operator is

$$\begin{aligned}
< E_{n'z}|z|1s > &= \frac{1}{\sqrt{3}}\frac{2(1+n'^2)^{1/2}}{(1-e^{-2\pi n'})^{1/2}}n'^2 \int dr\ r^2 \frac{1}{4r^2} 2e^{-r} r \left[\frac{1}{2\pi}\int e^{-2ir\xi/n'}(\xi+\frac{1}{2})^{-in'-2}(\xi-\frac{1}{2})^{in'-2}d\xi\right] \\
&= \frac{1}{4\pi\sqrt{3}}\frac{n'^2(1+n'^2)^{1/2}}{(1-e^{-2\pi n'})^{1/2}}\int(\xi+\frac{1}{2})^{-in'-2}(\xi-\frac{1}{2})^{in'-2}d\xi\int_0^\infty dr\ re^{-2ir\xi/n'}2e^{-r} \\
&= \frac{1}{4\pi\sqrt{3}}\frac{n'^2(1+n'^2)^{1/2}}{(1-e^{-2\pi n'})^{1/2}}\int d\xi \frac{-2}{(-i+2\xi/n')^2}(\xi+\frac{1}{2})^{-in'-2}(\xi-\frac{1}{2})^{in'-2}.
\end{aligned} \quad (16)$$

Putting

$$f(\xi) = \left(\xi+\frac{1}{2}\right)^{-in'-2}\left(\xi-\frac{1}{2}\right)^{in'-2}, \quad (17)$$

we have

$$\begin{aligned}
f'(\xi) &= \left(\xi+\frac{1}{2}\right)^{-in'-3}\left(\xi-\frac{1}{2}\right)^{in'-3} \times [(-in'-2)(\xi-1/2)+(in'-2)(\xi+1/2)] \\
&= \left(\xi+\frac{1}{2}\right)^{-in'-3}\left(\xi-\frac{1}{2}\right)^{in'-3}[-4\xi+in'].
\end{aligned} \quad (18)$$

A simple substitution gives

$$f'(\xi = n'i/2) = \frac{n'i2^6}{(n'+1)^3}e^{-2n'\tan^{-1}(1/n')}, \quad (19)$$

where use is made of the relation

$$\left(\frac{n'+i}{n'-i}\right)^{in'} = e^{-2n'\tan^{-1}(1/n')}. \quad (20)$$

Therefore, the contour integral is

$$\begin{aligned} I_C &= \int_C (\xi+\frac{1}{2})^{-in'-2}(\xi-\frac{1}{2})^{in'-2}\frac{2d\xi}{(1+i\frac{2\xi}{n'})^2} = -\frac{n'^2}{2}\left[-2\pi i\cdot in'\left(\frac{4}{n'^2+1}\right)^3 e^{-2n'\tan^{-1}\frac{1}{n'}}\right] \\ &= -\frac{\pi 2^6 (n')^3}{(n'^2+1)^3}e^{-2n'\tan^{-1}\frac{1}{n'}}. \end{aligned} \quad (21)$$

The matrix element is

$$\begin{aligned} < E_{n'z}|z|1s > &= \frac{n'^2}{4\pi\sqrt{3}}\frac{(1+n'^2)^{1/2}}{(1-e^{-2\pi n'})^{1/2}}\frac{\pi 2^6 n'^3}{(1+n'^2)^3}e^{-2n'\tan^{-1}\frac{1}{n'}} \\ &= \frac{2^4 n'^5}{\sqrt{3}(1+n'^2)^{5/2}}\frac{e^{-2n'\tan^{-1}\frac{1}{n'}}}{(1-e^{-2\pi n'})^{1/2}}. \end{aligned} \quad (22)$$

For $2s$ state, we consider

$$\begin{aligned} < 2s|z|n'p > &= (n')^{-3/2} < 2s|z|E_{n'z} > \\ &= (n')^{-3/2}\frac{n'^2[1+n'^2]^{1/2}}{4\pi\sqrt{3}(1-e^{-2\pi n'})^{1/2}} \\ &\times \int(\xi+1/2)^{-in'-2}(\xi-1/2)^{in'-2}d\xi\int dr\ re^{-2ir\xi/n'}\frac{1}{\sqrt{2}}(1-r/2). \end{aligned} \quad (23)$$

Noting that

$$\int dr\frac{1}{\sqrt{2}}e^{-r\left(\frac{1}{2}+i\frac{2\xi}{n'}\right)}(r-r^2/2) = \frac{1}{\sqrt{2}}\left(\frac{1}{a}-\frac{1}{a^2}\right), \quad (24)$$

where $a = \frac{1}{2}+\frac{2i\xi}{n'}$, we consider the integral

$$I_{C2} = \frac{1}{\sqrt{2}}\int_C\left(\xi+\frac{1}{2}\right)^{-in'-2}\left(\xi-\frac{1}{2}\right)^{in'-2}\left(\frac{1}{a^2}-\frac{1}{a^3}\right)d\xi. \quad (25)$$

A direct substitution of $\xi = in'/4$ into Eq. (18) gives $f'(\xi) = 0$. In order to find higher residues we compute the second order derivative of $f(\xi)$, of which the result is

$$f''(\xi) = 2(\xi+1/2)^{-in'-4}(\xi-1/2)^{in'-4}[10\xi^2-5in'\xi+(1-n'^2)/2]. \quad (26)$$

From this, we obtain

$$\begin{aligned} f''(\xi = in'/4) &= \frac{1}{4}(n'^2+4)\left(\frac{\xi-1/2}{\xi+1/2}\right)^{in'}\frac{1}{(\xi+1/2)^4(\xi-1/2)^4} \\ &= e^{-2n'\tan^{-1}\frac{2}{n'}}\frac{2^{14}}{(n'^2+4)^3}. \end{aligned} \quad (27)$$

Therefore, the residue calculus shows that

$$\begin{aligned} I_{C2} &= \int_C d\xi\ (\xi+1/2)^{-in'-2}(\xi-1/2)^{in'-2}(a^{-2}-a^{-3}) \\ &= -\frac{n'^3}{i^3 2^3}2\pi i\frac{1}{2!}\frac{2^{14}}{(n'^2+4)^3}e^{-2n'\tan^{-1}\frac{2}{n'}} \\ &= 2\pi\ \frac{2^{10}n'^3}{(n'^2+4)^3}\ e^{-2n'\tan^{-1}\frac{2}{n'}}. \end{aligned} \quad (28)$$

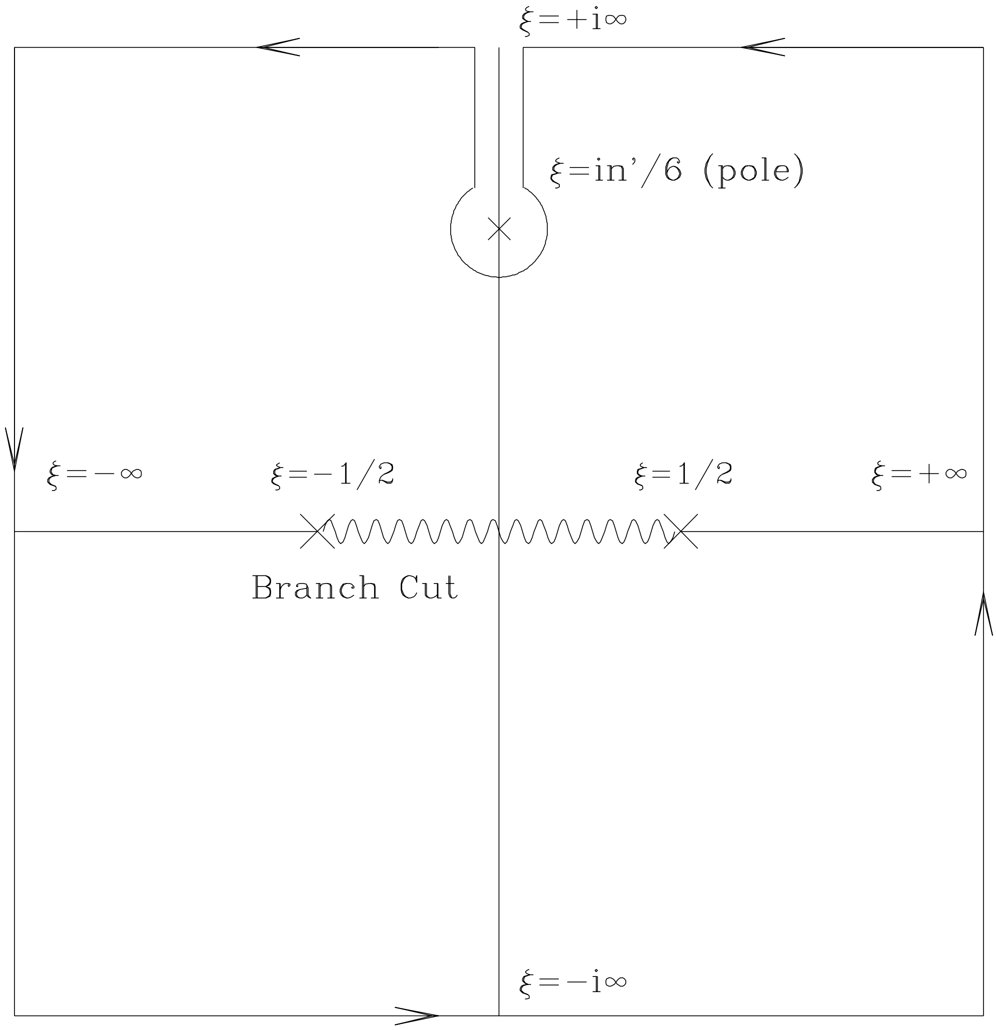

Fig. 2.— Contour for the integral for bound-free matrix elements. In particular in this figure the pole is for $\tau_{3s,n'p}$. For $\tau 1s, n'p$, the location of the pole is $\xi = in'/2n'$, and for $\tau_{2s,n'p}$ it is at $\xi = in'/4n'$

From this we immediately see

$$\begin{aligned} < 2s|z|n'z > &= (n')^{3/2} \frac{n'^2(1+n'^2)^{1/2}}{4\pi\sqrt{3}(1-e^{-2\pi n'})^{1/2}} \frac{2\pi}{\sqrt{2}} \frac{2^{10} n'^3 e^{-2n' \tan^{-1}\frac{2}{n'}}}{(n'^2+4)^3} \\ &= \frac{2^{17/2}(n')^{7/2}(1+n'^2)^{1/2} e^{-2n' \tan^{-1}\frac{2}{n'}}}{\sqrt{3}(n'^2+4)^3(1-e^{-2\pi n'})^{1/2}}. \end{aligned} \tag{29}$$

Now we compute the matrix elements for $3s - n'p$ transitions. We consider the radial wavefunction

$$R_{3s}(r) = \frac{2}{3\sqrt{3}} e^{-r/3} \left(1 - \frac{2}{3}r + \frac{2}{27}r^2\right). \tag{30}$$

We have to evaluate

$$\tau_{3s}^{n'z} = < 3s|z|n'z >= n'^{-3/2} < 3s|z|E_{n'}z >$$

$$= \frac{n'^{1/2}[1+n'^2]^{1/2}}{4\pi\sqrt{3}[1-e^{-2\pi n'}]^{1/2}} \int_C \left(\xi+\frac{1}{2}\right)^{-in'-2} \left(\xi-\frac{1}{2}\right)^{in'-2} d\xi \int_0^\infty dr\; re^{-\frac{2i\xi r}{n'}} \frac{2}{3\sqrt{3}} e^{-\frac{1}{3}r} \left(1-\frac{2}{3}r+\frac{2}{27}r^2\right). \tag{31}$$

First, we consider

$$\begin{aligned} I_1 &= \frac{2}{3\sqrt{3}} \int_0^\infty dr\; e^{-(\frac{1}{3}+\frac{2i\xi}{n'})r} \left(r-\frac{2}{3}r^2+\frac{2}{27}r^3\right) \\ &= \frac{2}{3\sqrt{3}} \int_0^\infty dr\; \left[\left(-\frac{\partial}{\partial\lambda}\right)-\frac{2}{3}\left(-\frac{\partial}{\partial\lambda}\right)^2+\frac{2}{27}\left(-\frac{\partial}{\partial\lambda}\right)^3\right] e^{-\lambda r} \\ &= \frac{2}{3\sqrt{3}} \left[\frac{1}{\lambda^2}-\frac{2}{3}\frac{2}{\lambda^3}+\frac{2}{27}\frac{6}{\lambda^4}\right] \quad \text{with} \quad (\lambda=\frac{1}{3}+\frac{2i\xi}{n'}). \end{aligned} \tag{32}$$

We set as before

$$f(\xi) = (\xi+1/2)^{-in'-2}(\xi-1/2)^{in'-2}. \tag{33}$$

From Eq. (26), the third derivative is

$$f^{(3)} = \left(\xi+\frac{1}{2}\right)^{-in'-5} \left(\xi-\frac{1}{2}\right)^{in'-5} \left[-120\xi^3+90in'\xi^2+18(n'^2-1)\xi+in'(\frac{7}{2}-n'^2)\right]. \tag{34}$$

The residue is

$$\begin{aligned} f^{(3)}(in'/6) &= \left(\xi+\frac{1}{2}\right)^{-in'-5} \left(\xi-\frac{1}{2}\right)^{in'-5} \left(\frac{1}{18}in'^3+\frac{1}{2}in'\right) \\ &= \left(\xi+\frac{1}{2}\right)^{-in'-5} \left(\xi-\frac{1}{2}\right)^{in'-5} \frac{in'}{18}(n'^2+9). \end{aligned} \tag{35}$$

The contour integral becomes

$$\begin{aligned} I_{C2} &= \int_C d\xi\; \left(\xi+\frac{1}{2}\right)^{-in'-2} \left(\xi-\frac{1}{2}\right)^{in'-2} \left(\frac{2}{27}\frac{6}{\lambda^4}-\frac{2}{3}\frac{2}{\lambda^3}+\frac{1}{\lambda^2}\right) \\ &= \frac{4}{9}\int_C \frac{f(\xi)d\xi}{(2i/n')^4(\xi-in'/6)^4} - \frac{4}{3}\int_C \frac{f(\xi)d\xi}{(2i/n')^3(\xi-in'/6)^3} + \int_C \frac{f(\xi)d\xi}{(2i/n')^2(\xi-in'/6)^2} \\ &= \frac{n'^4}{36}\frac{1}{3!}(-2\pi i)f^{(3)}(\xi=in'/6) - \frac{in'^3}{6}\frac{1}{2!}(-2\pi i)f^{(2)}(\xi=in'/6) + \frac{-n'^2}{4}(-2\pi i)f^{(1)}(\xi=in'/6) \\ &= -\frac{3\cdot 36^2 2\pi n'^3}{(n'^2+9)^4}(7n'^2+27)e^{-2n'\tan^{-1}\frac{3}{n'}}, \end{aligned} \tag{36}$$

where use is made of the relation

$$\xi^2-\frac{1}{4} = -\frac{n'^2}{36}-\frac{1}{4} = -\frac{1}{36}(n'^2+9). \tag{37}$$

Therefore, we have

$$\begin{aligned} \tau_{3s}^{n'p} &= \; < 3s \parallel r \parallel n'p >= \frac{n'^{1/2}(1+n'^2)^{1/2}}{4\pi(1-e^{-2\pi n'})^{1/2}} \frac{2}{3\sqrt{3}} \frac{-3\cdot 36^2 2\pi n'^3}{(n'^2+9)^4}(7n'^2+27)e^{-2n'\tan^{-1}\frac{3}{n'}} \\ &= \frac{-3\sqrt{3}12^2 n'^{7/2}(1+n'^2)^{1/2}(7n'^2+27)}{(1-e^{-2\pi n'})^{1/2}(n'^2+9)^4}\; e^{-2n'\tan^{-1}\frac{3}{n'}}. \end{aligned} \tag{38}$$

The radial wave function for the $3d$ state is given by

$$R_{3d}(r) = \frac{4}{81\sqrt{30}} r^2 e^{-\frac{r}{3}}. \tag{39}$$

We have

$$\begin{aligned}
\tau_{3d}^{n'z} &= <3d|z|n'z>= (n')^{-\frac{3}{2}} <3d|z|E_{n'z}> \\
&= \frac{n'^{1/2}(1+n'^2)^{1/2}}{4\pi\sqrt{3}(1-e^{-2\pi n'})^{1/2}} \int_C \left(\xi+\frac{1}{2}\right)^{-in'-2} \left(\xi-\frac{1}{2}\right)^{in'-2} d\xi \\
&\times \int_0^\infty dr\ re^{-\frac{2i\xi r}{n'}} \frac{4}{81\sqrt{30}} r^2 e^{-\frac{r}{3}}. \qquad (40)
\end{aligned}$$

Noting that

$$f^{(3)}(\xi = in'/6) = \frac{-2\cdot 36^4 n' i}{(n'^2+9)^4} e^{-2n'\tan^{-1}\frac{3}{n'}}, \qquad (41)$$

the contour integral is evaluated as

$$\begin{aligned}
I_{C3} &= \int_C \left(\xi+\frac{1}{2}\right)^{-in'-2} \left(\xi-\frac{1}{2}\right)^{in'-2} \frac{4}{81\sqrt{30}} \frac{6}{\lambda^4} d\xi \\
&= \frac{24}{81\sqrt{30}} \frac{n'^4}{16} \frac{1}{3!}(-2\pi i) f^{(3)}\left(\xi = \frac{in'}{6}\right) \\
&= \frac{-n'^5}{9\sqrt{30}} \frac{4\pi 36^3}{(n'^2+9)^4} e^{-2n'\tan^{-1}\frac{3}{n'}}. \qquad (42)
\end{aligned}$$

Therefore, the matrix element is given by

$$\begin{aligned}
\tau_{3d}^{n'z} &= <3d|z|n'z>= \frac{n'^{1/2}(1+n'^2)^{1/2}}{4\pi\sqrt{3}(1-e^{-2\pi n'})^{1/2}} \frac{-n'^5}{9\sqrt{30}} \frac{4\pi 36^3}{(n'^2+9)^4} e^{-2n'\tan^{-1}\frac{3}{n'}} \\
&= -\frac{12^3}{\sqrt{10}} \frac{n'^{11/2}(1+n'^2)^{1/2}}{(n'^2+9)^4(1-e^{-2\pi n'})^{1/2}} e^{-2n'\tan^{-1}\frac{3}{n'}}. \qquad (43)
\end{aligned}$$

(c) Cross Sections

In this subsection, we present the cross sections obtained with a simple code incorporating the matrix elements described in the previous subsections. Dividing the sum in Eq. (1) into a sum over bound states and an integral over free states, the scattering cross section is given by

$$\sigma/\sigma_{Th} = \left(\frac{\omega\omega'^3}{\omega_L^2}\right) \left|\sum_{n=2}^\infty \tau_{2s,np}\tau_{1s,np}\left(\frac{1}{\omega_{n1}-\omega}+\frac{1}{\omega_{n1}+\omega'}\right) + \int dn' \tau_{2s,n'p}\tau_{1s,n'p}\left(\frac{1}{\omega_{n'1}-\omega}+\frac{1}{\omega_{n'1}+\omega'}\right)\right|^2. \qquad (44)$$

Here, $\sigma_{Th} = 0.665\times 10^{-24}$ cm^2 is the Thomson scattering cross section, and ω_L is the angular frequency corresponding to the Lyman limit.

Near resonance $\omega - \omega_{N1} = \Delta\omega \ll \omega$ with the Np state the dominant contribution is made by this single term. If $\Delta\omega$ is still larger than the damping term, then the cross section is approximately given by

$$\sigma_{nr}/\sigma_{Th} \simeq \left(\frac{\omega\omega'^3}{\omega_L^2}\right)\left(\frac{\tau_{2s,Np}\tau_{1s,Np}}{\omega_{N1}-\omega}\right)^2 \propto \Delta\omega^{-2}. \qquad (45)$$

This is the origin of the Hα wing profile, if the wing is formed from Raman scattering of flat UV radiation around Lyβ (e.g. Lee 2000). As is pointed out by Skopal (2006) the wing profiles proportional to $\Delta\omega^{-2}$ are also formed from optically thin fast winds.

Very near the resonance, the scattering cross section is excellently described by a Lorentzian, as is well known in standard text book on radiation. Due to the resonance nature, the scattering cross section ranges a large orders of magnitude. In particular, He II emission lines arising from states with even principal quantum numbers to $2s$ state possess a large scattering cross section compared with other metallic lines such as O VI 1032, 1038.

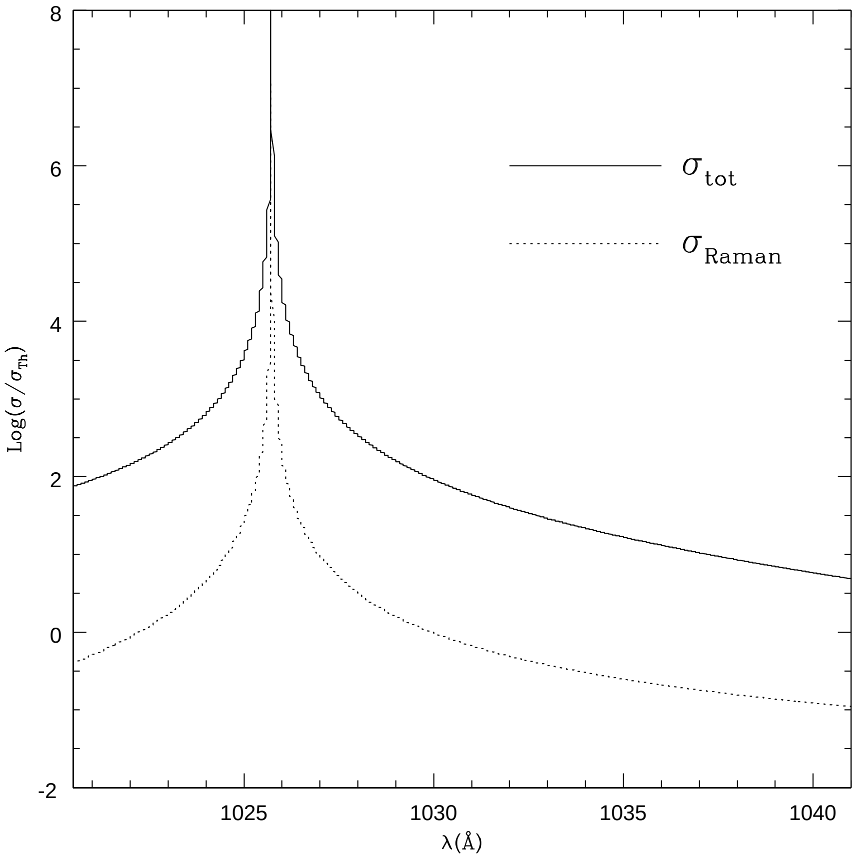

Fig. 3.— Cross sections around Lyβ in units of the Thomson scattering cross section σ_{Th}. The total cross section σ_{tot} is the sum of Raman scattering cross section and Rayleigh scattering cross section.

III. OBSERVATIONAL RAMIFICATIONS

Spectropolarimetry is particularly important in the case of Raman scattering, because the Raman scattered feature is composed of purely scattered radiation without being mixed with the incident radiation that is usually unpolarized and reduces the degree of polarization.

Thus far, Raman scattering by atomic hydrogen is unique features to symbiotic stars and young planetary nebulae. It may be worthy to consider other class of objects that may harbor a thick neutral region in the vicinity of a strong UV radiation source.

One may consider the broad emission line region in active galactic nuclei. In active galactic nuclei, broad emission line region is photoionized by strong UV radiation. In a typical active galactic nuclei, a neutral region near equatorial plane is often invoked by the unified model in order to hide the central region from direct views for low latitude observers. Type 2 active galactic nuclei no apparent broad permitted lines in their UV and optical spectra and characterized by high X-ray hardness may be identified with normal active galactic nuclei in the unified model.

However, the deep gravitational potential due to the supermassive black hole giving rise to broad spectral width may easily hide the Raman scattered component. Due to the spectral broadening by the factor λ_o/λ_i, the Raman scattered features will appear abnormally broad. These components may be detected more readily using

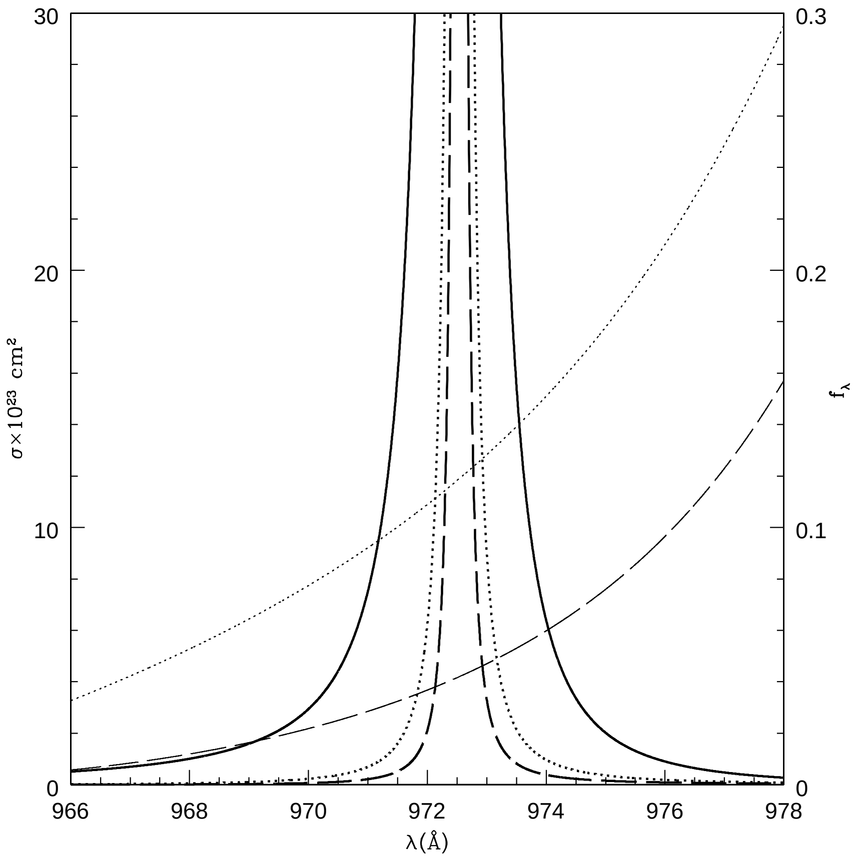

Fig. 4.— Cross sections around Lyγ in units of 10^{-23} cm^2 and branching ratios. The thick solid line shows the total scattering cross section, the thick dotted line represents the scattering cross section into the level $2s$ (for He II λ 4850) and the thick dashed line represents the sum of the scattering cross sections into the levels $3s$ and $3d$.

spectropolarimetry, where direct unpolarized radiation is filtered out. Lee & Yun (1998) computed polarized Hα via Raman scattering in active galactic nuclei. It is quite interesting that narrow line radio galaxy Cyg A exhibits enormously broad polarized Hα from Keck spectropolarimetry (Ogle et al. 1997).

Another interesting class of objects in which Raman scattering may be relevant is premain sequence stars. Stars are formed in giant molecular cloud via gravitational collapse. The necessity of angular momentum transport outwards leads to formation of a disk and a jet, and various shocks. Hα emission is an important signature of these objects, which requires the presence of an ionized region.

It will be also challenging for solar physicists. The solar prominence appear in regions where neutral hydrogen density is $N_{HI} \sim 10^{20}$ cm^{-2}, where He II photons can be easily Raman scattered. A fast and high resolution spectrograph will be quite useful to this observation, which yield much information about the relative geometry of ionized and neutral material in the solar surface.

ACKNOWLEDGMENTS

The author gratefully acknowledges financial support from the Astrophysical Research Center of the Structure and Evolution of the Cosmos (ARCSEC) funded by the Korea Science and Engineering Foundation (KOSEF).

REFERENCES

Allen, D. A., On the unidentified bands 6830, 7088 in symbiotic stars, 1980, MNRAS, 190, 75

Bethe, H., & Salpeter, E. E., 1957, Quantum Mechanics of One and Two Electron Atom, Academic Press, New York

Birriel, J. J., Raman-Scattered He II at 4851 in the Symbiotic Stars HM Sagittae and V1016 Cygni, 2004, ApJ, 612, 1136

Groves, B., Dopita, M. A., Williams, R. E.; Hua, C.-T., The Internal Extinction Curve of NGC 6302 and its Extraordinary Spectrum, 2002, PASA, 19, 425

Harries, T. J. & Howarth, I. D., Raman scattering in symbiotic stars. I. Spectropolarimetric observations, 1996, A&AS, 119, 61

Jung, Y.-C. & Lee, H. -W., Centre shift of the Raman scattered He II 4850 in the symbiotic star V1016 Cygni, 2004, MNRAS, 355, 221

Karzas, W. J. & Latter, R., Electron Radiative Transitions in a Coulomb Field, 1961, ApJS, 6, 167

Lee, H. -W., Raman-Scattering Wings of H alpha in Symbiotic Stars, 2000, ApJ, 541 L25

Lee, H. -W., Jung, Y.-C., Song, I.-O., Ahn, S.-H., Raman-scattered He II 4850, 6545 in the Young and Compact Planetary Nebula IC 5117, 2006, ApJ, 636, 1045

Lee, H. -W., & Lee, K. W., On the profiles and the polarization of Raman-scattered emission lines in symbiotic stars, 1997, MNRAS, 287, 211

Lee, H. -W., & Park, M. -G., Toward the Evidence of the Accretion Disk Emission in the Symbiotic Star RR Telescopii, 1999, ApJ, 515, L89

Lee, H. -W., & Yun, J. -H., On the polarization of H alpha scattered by neutral hydrogen in active galactic nuclei, 1998, MNRAS, 301, 193

Nussbaumer, H., Schmid, H. M., & Vogel, M., Raman Scattering as a Diagnostic Possibility in Astrophysics 1989, A&A, 211, L27

Ogle, P. M., Cohen, M. H., Miller, J. S., Tran, H. D., Fosbury, R. A. E., Goodrich, R. W., Scattered Nuclear Continuum and Broad H alpha in Cygnus A, 1997, ApJ, 482, L37

Péquignot, D., Baluteau, J.-P., Morisset, C., & Boisson, C., NGC7027:discovery of a Raman line in a planetary nebula., 1997, A&A, 323, 217

Sakurai, J. J., 1967, Advanced Quantum Mechanics, Addison-Wesley, Reading, MA

Saslow, W. M., & Mills, D. L., Raman Scattering by Hydrogenic Systems, 1969, Phys. Rev., 187, 1025

Schmid, H. M., Identification of the Emission Bands at 6830 Å and 7088 Å, 1989, A&A, 211, L31

Schmid, H. M., Raman Scattering and Symbiotic Stars, 2001, Eta Carinae and Other Mysterious Stars: The Hidden Opportunities of Emission Spectroscopy, ASP Conference Proceedings, Vol. 242. Edited by Theodore R. Gull, Sveneric Johannson, and Kris Davidson. San Francisco: Astronomical Society of the Pacific, 347

Schmid, H. M., & Schild, H., Raman scattered emission lines in symbiotic stars: A spectropolarimetric survey, 1994, A&A, 281, 145

Schild, H & Schmid, H. M., Spectropolarimetry of symbiotic stars. On the binary orbit and the geometric structure of V1016 Cygni, 1996, A&A, 310, 211

Skopal, A., Broad H alpha wings from the optically thin stellar wind of the hot components in symbiotic binaries, 2006, A&A, 457, 1003

van Groningen, E., Further Evidence for Raman Scattering in RR Telescopii 1993, MNRAS, 264, 975

Zhang, Y., Liu, X. -W., Luo, X. -G., Péquignot, D., Barlow, M. J., Integrated spectrum of the planetary nebula NGC 7027, 2005, A&A, 442, 249